

Analysis of Radial Force as a Source of Vibration in an Induction Motor with Skewed Slots

D. H. Im, J. H. Chang, S. C. Park and B. I. Kwon

Dept. of Electrical Engineering, Hanyang University, Seoul 133-791, Korea

J. P. Hong

Dept. of Electrical Engineering, Changwon Nat'l University, Changwon 641-773, Korea

B. T. Kim

CAD/CAM Lab., Samsung Electro-mechanics Co., Suwon 441-743, Korea

Abstract - This paper presents a method to analyze radial force densities acting on each stator tooth of an induction motor with skewed slots. Two-dimensional finite element method is used for electromagnetic field analysis of an induction motor, and skew effects are considered by coupling several disks cut by planes perpendicular to the shaft. Radial force densities as a source of vibration are calculated along the surface elements of each stator tooth and its time harmonics are examined by discrete Fourier decomposition.

I. INTRODUCTION

In an electric motor, mechanical vibrations of electromagnetic origin are generated by the fluctuations of magnetic forces applied on the stator. Particularly, these phenomena are serious when the forcing frequencies match one or more of the structural frequencies in the machine. Thus, accurate determinations of the exciting radial magnetic forces are essential in vibration analysis.

One technical approach solving magnetic field is sinusoidal method, in which magnetic vector potential A , and current density J varies sinusoidally with time. But, this is not adequate to represent space and time harmonics of surface forces acting on stator teeth. The method that has been developed in this paper is a step-by-step method, with two different reference frames, one fixed with stator, the other one moving with the rotor.

In order to have a good evaluation of the distributions of magnetic forces along the stator, forces exerted on teeth and on conductors are evaluated. However, the relative magnitudes of the force densities acting on the teeth are much greater compared with conductors [1]. Thus, only radial force densities are calculated along the surface elements of the teeth by the Maxwell's stress tensor method. The time dependence of the field and the motion of the rotor are modelled by the backward-difference scheme.

II. FIELD ANALYSIS

A three-dimensional formulation should be used to calculate the magnetic field of an induction motor. But, their practical applications are still restricted to relatively simple geometries. So, two-dimensional model is used in this paper and the three dimensional effects such as the skew of rotor slots, and end-region fields are taken into account within the two-dimensional model.

Simulations are carried out for a 150 kW squirrel cage induction motor with 6 poles, 72 stator slots, 60 rotor bars, as shown in Fig. 1.

A. Field Equation

The magnetic vector potential form of the Maxwell's equation is written as

$$\nabla \times (\nu \nabla \times \mathbf{A}) - J_{ext} + \sigma \frac{\partial \mathbf{A}}{\partial t} + \sigma \nabla \phi = 0, \quad (1)$$

where \mathbf{A} , ν , σ are the magnetic vector potential, the reluctivity of the material and the electrical conductivity, respectively, and J_{ext} is the current density provided by an external power supply. ϕ represents the electric scalar potential.

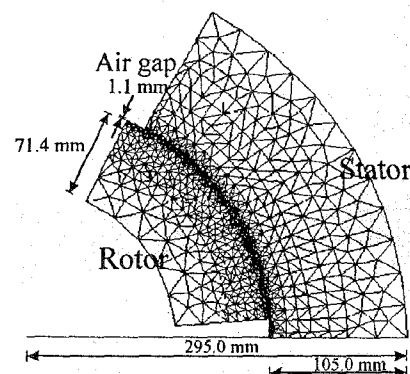


Fig. 1. Analysis Model

The gradient of scalar potential ϕ can be expressed with the aid of the potential difference induced between the ends of a rotor bar.

B. Circuit Equations

To analyze a voltage fed induction motor, field equations must be coupled with circuit equations. Thus, the impedance of the end-rings and the end-windings must be introduced. These quantities are computed analytically and will supplement the two-dimensional finite element analysis with skewing model.

1) Stator equation : If we let R and L_0 , the analytically computed resistance of stator winding per phase and inductance of the end-windings, respectively, the following equation is obtained on the stator winding.

$$V_s = RI_s + L_0 \frac{dI_s}{dt} + \frac{d\phi}{dt} \quad (2)$$

where ϕ is the linkage flux in the winding and will be expressed by magnetic vector potential A .

2) Rotor equation : The rotor cage bars are solid conductors connected together by end rings, and can be described by a polyphase circuit.

The details of the construction of the circuit equations are presented in [2],[3].

C. Time-Dependence

A time-dependent field is solved by discretizing the time at short time intervals. In the backward difference scheme, the time derivatives of the vector potential and the current are approximated to

$$\frac{\partial A}{\partial t} = \frac{A_{t+\Delta t} - A_t}{\Delta t} \quad (3)$$

$$\frac{\partial I}{\partial t} = \frac{I_{t+\Delta t} - I_t}{\Delta t} \quad (4)$$

D. Skew-Modelling

An approach to represent a skewed rotor in two dimensions is to use a set of unskewed models, cut by planes perpendicular to the shaft as shown in Fig.2.

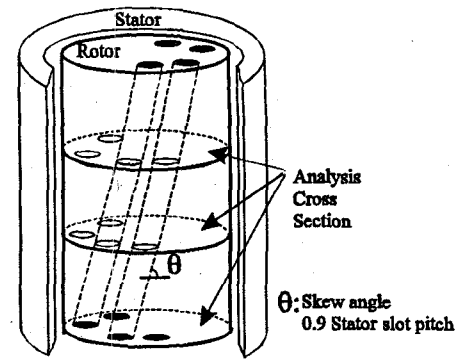


Fig. 2. Skew model

Indeed, a real skewed machine is fabricated from a stack of straightened-punched laminations, each of which may be regarded as a single unskewed slice.

The magnetic field of each slice is coupled together in one matrix form satisfying the continuity of stator and rotor bar currents.

E. Motion of Rotor

The rotor must be rotated by the angle corresponding to mechanical angle associated with motion equation at each time step. However, in this paper, the motor operates at a constant speed and the rotor movement at each time step is modelled by sliding surface technique, in which potentials on the two sides of sliding surface are equal.

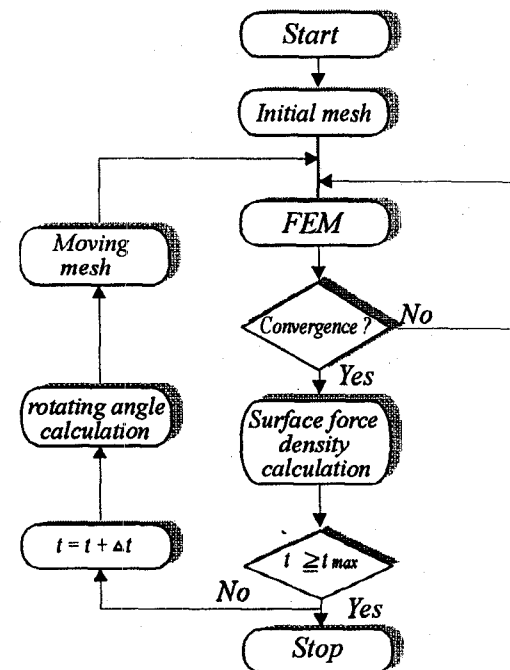


Fig. 3. Flow chart of dynamic analysis

III ANALYSIS OF RADIAL FORCE DENSITIES

A. Computation Method

The surface force density derived from the Maxwell tensor formulation has the following expression for the ferromagnetic material [4].

$$F_s = [H_1 (B_1 \cdot n_{12}) - (B_1 H_1 / 2) n_{12}] - [H_2 (B_2 \cdot n_{12}) - (B_2 H_2 / 2) n_{12}] , \quad (5)$$

where H_i is the magnetic field intensity and B_i is the flux density of surface element adjacent to the boundary. n_{12} is unit normal vector to the surface and goes to airgap region from the higher permeability region as shown in Fig.4.

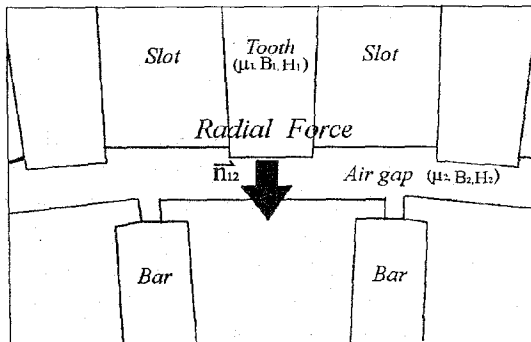


Fig. 4. Surface force density calculation

B. Frequency Analysis

A discrete Fourier decomposition of the radial force densities in each surface element of every stator teeth has the following form :

$$F(\omega t) = \frac{a_0}{2} + \sum_{n=1}^{N/2-1} (a_n \cos n\omega t + b_n \sin n\omega t) , \quad (6)$$

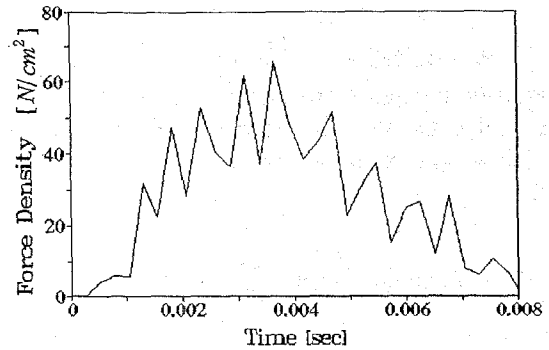
$$a_0 = \frac{2}{N} \sum_{i=1}^N F(\omega t_i) , \quad a_n = \frac{2}{N} \sum_{i=1}^N F(\omega t_i) \cos n\omega t_i ,$$

$$b_n = \frac{2}{N} \sum_{i=1}^N F(\omega t_i) \sin n\omega t_i , \quad (n=1, 2, \dots, \frac{N}{2}-1).$$

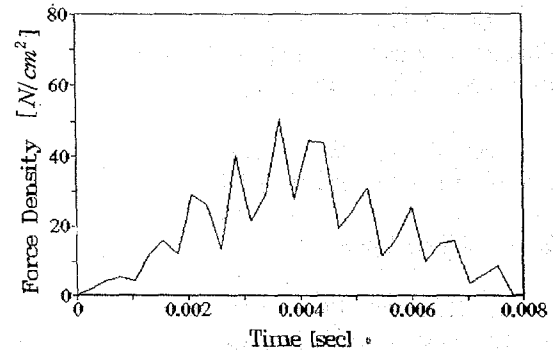
In (6), N is 64, the double number of time step used for one period of the surface force function corresponding to 180 electrical degrees. The fundamental frequency of the magnetic force is equal to twice the current frequency, f_c (60 Hz).

C. Simulation Results

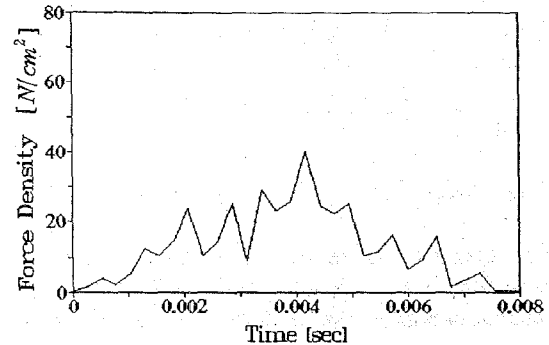
Fig. 5 shows the time evolution of the radial force densities applied on a tooth of each slice of the stator. It can be seen that the radial force density at each slice in the skewed model is shifted corresponding to skew angle. The force densities calculated during the computation represent the instantaneous values at each point in time, and appear as non-sinusoidal variation periodic in half period of current frequency f_c . The modulations due to the presence of slots are obvious.



(a) 1st slice



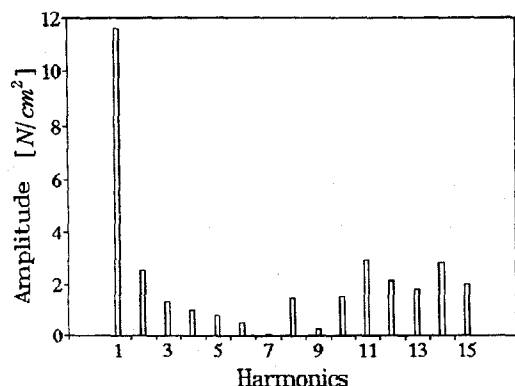
(b) 2nd slice



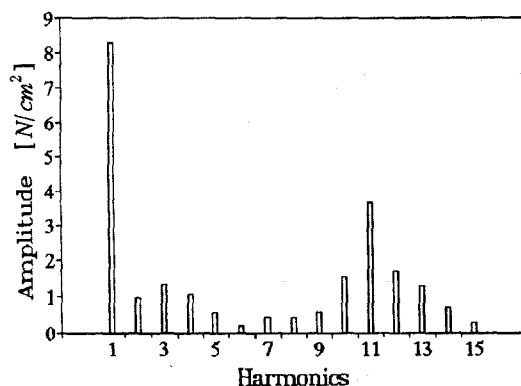
(c) 3rd slice

Fig. 5 Radial force densities on a tooth as a function of time

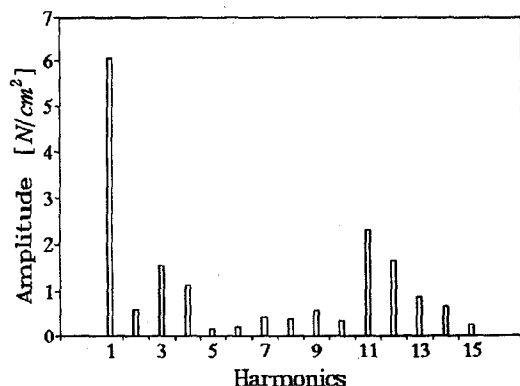
In Fig. 6, surface force time dependent functions are decomposed by discrete Fourier decomposition in a stator tooth surface elements at each slice. The frequency spectra of the radial force densities acting on the same tooth in the shaft direction are different because of the skewed rotor bars effect. Table I. shows the quantities of these radial force harmonics at each slice tooth surface. The force harmonics was investigated up to 30th, i.e. 1,800 [Hz] since the mechanical resonance frequency of stator are usually below about 2,000[Hz].



(a) 1st slice



(b) 2nd slice



(c) 3rd slice

TABLE I. Characteristics of radial force harmonics

Harmonics order	Frequencies [Hz]	Radial force densities [N/cm ²]		
		1st slice	2nd slice	3rd slice
2	120	11.601	8.297	6.071
4	240	2.555	0.989	0.587
6	360	1.348	1.348	1.548
8	480	0.985	1.073	1.126
10	600	0.788	0.570	0.148
12	720	0.501	0.191	0.207
14	840	0.067	0.427	0.406
16	960	1.469	0.434	0.369
18	1080	0.243	0.572	0.567
20	1200	1.522	1.525	0.344
22	1320	2.897	3.682	2.316
24	1440	2.118	1.725	1.646
26	1560	1.786	1.288	0.865
28	1680	2.797	0.754	0.637
30	1800	1.979	0.286	0.255

V. CONCLUSION

In this paper, the radial force densities acting on teeth of an induction motor with skewed slots, as a source of stator mechanical vibration, are calculated and its harmonics are analyzed by discrete Fourier decomposition. As a result, if the mechanical resonance frequencies of the stator are known at the stage of motor design, we can get rid of the radial force harmonics which match one of the resonance frequencies by adjusting skew angle of rotor bar.

REFERENCES

- [1] Y. Lefevre et al, "Determination of synchronous motor vibrations due to electromagnetic force harmonics". IEEE Trans on Magnetics, Vol. 25, No. 4, pp. 2974- 2976, 1989.
- [2] A. Arkkio, *Analysis of induction motors based on the numerical solution of the magnetic field and circuit equations*. Helsinki 1987, Acta Polytechnica Scandinavica, Electrical Engineering Series No. 59.
- [3] E. Vassent et al, "Simulation of induction machine operation using a step by step finite element coupled with circuits and mechanical equations". IEEE Trans on Magnetics, Vol. 27, No. 6, pp. 5232-5234, 1991.
- [4] G. Henneberger et al, "Procedure for the numerical computation of mechanical vibrations in electrical machines". IEEE Trans on Magnetics, Vol. 28, No. 2, pp. 1351-1354, 1992.

Fig. 6. Discrete Fourier decomposition of the radial forces densities